Cycles of Andean Mountain Building Archived in the Amazon Fan

Cody Mason (cmason@westga.edu)
University of West Georgia https://orcid.org/0000-0003-4065-3535
Brian Romans
Virginia Tech
Molly Patterson
Binghamton University
Daniel Stockli
University of Texas at Austin
Andrea Fildani
The Deep Time Institute

Article

Keywords:

Posted Date: October 11th, 2021

DOI: https://doi.org/10.21203/rs.3.rs-798408/v1

Version of Record: A version of this preprint was published at Nature Communications on November 15th, 2022. See the published version at https://doi.org/10.1038/s41467-022-34561-6.

Abstract

Detrital zircons (DZs) in terrigenous sediment recovered from the late Pleistocene Amazon Fan have distinct modes of U-Pb crystallization ages and U-Th/He (ZHe) cooling ages that correlate to known South American magmatic and tectonic events. Young ZHe age modes record two phases of Andean exhumation, a late Cretaceous – Paleogene phase, and a late Miocene phase containing the highest density of ZHe age data. Nearly 40% of DZs were found to have Cenozoic ZHe ages, suggesting that the Andes are the main source of clastic detritus in the Amazon Fan. However, Andean upland sediment sources evidently contain a deep-time thermal record of mountain building. Neoproterozoic and early Paleozoic ZHe ages broadly delineate the Cambro-Ordovician Pampean and Famatanian orogenies between ~ 600–400 Ma, while a late Carboniferous to early Permian ZHe age mode (~ 275–300 Ma) likely represents a Paleozoic phase of the Gondwanan orogeny or magmatic arc activity and exhumation along the proto-Andean margin. An ~ 175–225 Ma ZHe mode records Late Triassic – Early Jurassic subduction related magmatism and deformation along the western margin of South America. We also find evidence for recycling and recent exhumation of craton aged DZs, possibly related to the broad drainage reversals experienced by the Amazon River. The first frequency analysis of detrital ZHe age data from the Amazon Fan results in two periods of crustal cooling, one at 57 Ma and another at 92 Ma (90% and 85% confidence, respectively). We attribute this periodicity in ZHe cooling age data to upper and lower plate coupling along the subduction dominated western margin of South America—and more specifically to cycles of orogenesis that include phases of magmatism, orogenic relief construction, and later destruction.

Introduction

Globally, cordilleran systems with volcanic arcs exhibit episodic cycles of magmatism, which are often constrained by the measurement of U-Pb ages of zircons in igneous and detrital material (Paterson and Ducea, 2015). Conceptual models link episodic magmatism in cordilleran arc systems to a suite of related processes in the mantle and upper plate, including tectonic activity in the orogen, and resulting surface processes (DeCelles et al., 2015). For example, one version of the orogenic cycle is hypothesized to consists of periods of high magmatic flux associated with underthrusting of melt-fertile lower crust, delamination of a dense mafic orogenic root from the upper plate, and subsequent rapid isostatic uplift, tectonic growth of the fold-thrust belt, and increased orogen relief and enhanced erosion rates (DeCelles et al., 2009; 2015). Datasets of multiple thermochronometers from clastic detritus have previously been used to propose anti-correlation between the timing of magmatic flux events, and tectonic denudation of an orogen (Carrapa and DeCelles, 2015). And while orogenic cycles are proposed to occur at quasi-periodic timescales of ~25 – 50 Myr (DeCelles et al., 2009; 2015), or ~70 Myr (Sundell et al., 2019a), the nature and timing of erosional response to orogenic cycles are still unclear. Thermal events in the orogenic belt are preserved in the detritus shed from cordilleran systems into their associated basins (Reiners and Brandon, 2006), and, in some cases, ultimately transferred to passive margin marine stratigraphic archives (Mason et al., 2019; Fildani et al., 2016).

Deep-sea fans – large accumulations dominated by terrigenous sediment – record the physical and chemical signatures of their linked continent-scale river catchments (Hessler and Fildani, 2019). The Amazon Fan, offshore NE South America (Fig. 1), contains sediments that originated throughout its catchment, with a predominance of detritus sourced from the central and northern Andes (McDaniel et al., 1997; Mason et al., 2019). Since this terrigenous detritus records the tectonic history of the catchment, it may be useful in the recovery of cyclic thermal events. Furthermore, the application of low-temperature detrital thermochronometry could help clarify the tempo of magmatic and thermal events experienced by South America's active western margin over numerous timescales. Thus the sediment of the Amazon Fan represents an excellent record to examine thermal histories of detritus shed from within the Amazon Basin, including the Andes and its predecessor subduction-related orogenic systems.

Here, we characterize the thermotectonic histories experienced by detrital zircons (DZs) found in the late Pleistocene Amazon Fan through the application of combined DZ U-Pb and U-Th/He double dating (U-Pb/ZHe double dating; n = 114 individual DZs). We perform a frequency analysis of ZHe data, and present the detrital geochronologic and frequency analysis results in the context of: (1) provenance interpretations of Amazon Fan sediment, and (2) past orogenic events of the South American continent, including generation of zircons during phases of magmatism, and low-temperature cooling histories of zircons associated with periodic increases in cooling of crustal material associated with exhumation of the Andes.

Tectonic History And Detrital Zircon Provenance Of The Amazon River Catchment And Deep-sea Fan

Western South America is dominated by the high-elevation, cordilleran system formed through the subduction of oceanic lithosphere, arc volcanism, and deformation of the overlying South American plate. The orogenic system is divided, from west to east, into a forearc region consisting of a western cordillera containing the magmatic arc, and a retroarc region, consisting of an eastern cordillera, in the case of the central Andes a broad high-elevation plateau, and an active retroarc fold thrust belt (Horton, 2018a).

The recent phase of Andean orogenesis initiated due to subduction of the Nazca plate beneath the South America plate during the late Mesozoic, and may have progressed in time from the northern Andes toward the central and southern Andes (Chen et al., 2019). During the Paleogene, rates of shortening in the central Andes increased dramatically (Armijo et al., 2015; and references therein; Horton, 2018b), as did the elevation of the central Andes (McQuarrie et al., 2008) culminating in the Miocene with rise of the central Andean Plateau (Garzione et al., 2008; Sundell et al., 2019b). Andean retroarc foreland basin fill records increased accommodation and initiation of widespread coarse grained sedimentation starting in the Late Cretaceous to early Paleogene, and is interpreted to be the signal of shortening induced lithospheric flexure (Horton, 2018a and references therein). A geographically widespread hiatus or cessation of coarse grained sedimentation occurred across the Eocene, with renewed coarse grained sedimentation recorded in retroarc foreland basins starting in the Oligocene.

Subduction related deformation along the Pre-Andean margin was poly-cyclic, long lived and regional in extent (Chew, 2016). Early orogenic events experienced by western South America are the Neoproterozoic through Paleozoic assembly of Gondwana, including the Pan African-Brasiliano (Neoproterozoic), the Pampean (~Cambrian) and the Famatinian (~Ordovician) orogenies, respectively (Ramos et al., 2018; Chew et al., 2016). These widespread events were followed by phases of Permian-Triassic metamorphism (Chew, 2016), and Jurassic magmatism along the western margin of South America (Kontak et al., 1990). During the Mesozoic, prior to widespread Andean shortening, extension and post-rift thermal subsidence were the dominant modes of lithospheric deformation along much of the central Andes (Horton, 2019b), leading to the formation of large sedimentary basins along strike in the Cretaceous (Horton, 2018a).

Andean streams are tributaries to the Amazon River, which transfers clastic detritus from a wide array of lithologies, representing a large span of geologic time, depositional environments, and igneous and metamorphic facies (Chew et al., 2011). Northern Andean streams with high elevation headwaters in southern Columbia and Ecuador tap into an active volcanic arc, Paleogene and Cretaceous sedimentary units, and Neoproterozoic metamorphic units, Triassic metamorphic, and Jurassic volcanic and plutonic units in the retro arc fold-thrust belt (Jackson et al., 2019; Gomez Tapias et al., 2019).

A magmatic gap related to Peruvian flat slab subduction exists between ~2° – 15° S (Bernal et al., 2002; Gomez Tapias et al., 2019). There, Andean streams in Peru tap Mesozoic and Paleozoic sedimentary, volcanic, and metamorphic units in the eastern cordillera, and Cenozoic, Cretaceous, and Jurassic sedimentary units in the fold-thrust belt (Gomez Tapias et al., 2019). South of ~15° S, in the western cordillera of Peru, lies an active volcanic arc. However, most volcanic detritus is transferred to internally drained, high elevation basins within the Altiplano of Peru and Bolivia. The eastern cordillera, and fold-thrust belt of southern Peru and Bolivia are dominated by Cenozoic, late Mesozoic, and extensive Paleozoic sedimentary units (Gomez Tapias et al., 2019).

The modern east-flowing Amazon River is a relatively recent feature. An ancestral Amazon River once flowed east to west, supplying sediment from the craton to Andean retroarc foreland basins, until a phased reversal was completed in the Miocene, as marked by the transfer of Andean detritus to the Atlantic Ocean (Hoorn et al., 2017). Consequently, DZ age spectra of sediment from modern rivers of the Amazon system display evidence for recycling of zircons originally sourced from the craton (Pepper et al., 2016; Mason et al., 2019; Capaldi et al. 2017; Jackson et al., 2019). Specifically, modern river sediments from the Andes may contain DZs with age components related to the Meso-Neoproterozoic Sunsás orogen (Grenville equivalent), the Neoproterozoic to Cambro-Ordovician Famatinian – Pampean orogens, and U-Pb ages related to periods of Mesozoic through Cenozoic magmatic arc activity along western South America (Horton et al., 2015; Capaldi et al., 2017). DZs with U-Pb ages >1300 Ma correspond to cratonic terranes and are documented in modern Andean sourced rivers and in bedrock sources within the northern to central Andes (George et al., 2019). Pampean aged DZs are sometimes referred to as Pan African – Brasiliano, an orogeny that affected eastern South America, and which can also be found in modern Andean streams. The provenance of DZs in the lower Amazon River and Fan becomes difficult to discern because of the these recycled cratonic zircons from the Andes, which mix with concomitant aged craton-derived zircons eroded en-route to the coast (Mason et al., 2019). We address this issue with the application of double dating of DZs, where recent tectonic exhumation may be revealed by the low-temperature cooling history of cratonic aged DZs sourced from the Andes.

Onshore, catchments within the Amazon Basin draining high relief mountainous areas represent a small fraction of the total Amazon drainage basin area (~12%; Gibbs, 1967), yet contribute a disproportionate amount of sediment to the Amazon fluvial system and related deep-sea fan (Fig. 1). Cosmogenic nuclide concentrations of river sediment show that Andean sourced rivers have erosion rates an order of magnitude higher than Amazon lowland rivers, over multi-millennial timescales (See Fig. 1; Wittman et al., 2011). Direct observations of river suspended sediment loads (Meade et al., 1979), mud geochemistry from the Amazon Fan (McDaniel et al., 1997), and DZ provenance estimates along the lower Amazon River and deep-sea Fan suggest that a large proportion of sediment (~80 – 90%) may be sourced from the Andes (Mason et al., 2019). Given the source of sediment in the Amazon Fan is largely from the cordilleran system, the Amazon Fan sedimentary record should preserve the long thermal history of the tectonically active western margin of South America.

Double Dating (U-pb And U-th/he) Of Amazon Fan Detrital Zircons

DZ U-Pb ages are rarely reset during multiple phases of orogenesis, hindering interpretations of geologically recent and shallow exhumation histories (<5 km). Although quantitative mixture models applied to DZ age spectra have improved sediment provenance interpretations in the Amazon and other systems (Mason et al., 2017; Fildani et al. 2018; Mason et al., 2019; Blum et al., 2018), double dating of DZs significantly improves the interpretations of provenance, and more so, the geologically recent thermotectonic histories experienced by DZs (Reiners et al., 2005; Campbell et al., 2005; Fildani et al., 2016; Thomson et al., 2017; Odlum et al., 2019; Odoh et al., 2019).

ZHe thermochronology exploits the thermal diffusivity of ^{4}He in zircon produced by radiogenic decay of ^{238}U, ^{235}U and ^{232}Th. At high temperatures (> ~200° C), zircons do not retain measurable amounts of ^{4}He; once a zircon is advected through its closure temperature range (or the partial retention zone; 140° – 200° C), the zircon will begin to retain ^{4}He in measurable amounts that are a function of He diffusion kinetics and time since passage through the closure temperature. While U-Pb ages record primary crystallization from magmatic sources, U-Th/He dating of individual zircons yields information about the most recent exhumation history experienced by a zircon.

We measured 114 ZHe cooling ages in previously dated (U-Pb) DZs from the Amazon Fan (Fig. 1B). Selection of DZs for double dating was based on U-Pb age criteria; importantly, we sought to produce a representative characterization of cooling histories of detritus from the Amazon basin by measuring ZHe cooling ages in similar proportions to previously defined U-Pb age distributions from the Pleistocene Amazon Fan (see Fig. 1B) (Mason et al., 2019). DZs for double dating were further screened based on morphology suitable for the ZHe technique (Wolf and Stockli, 2010; Hart et al., 2016). DZs were selected from five samples of turbiditic sands collected from two sediment cores recovered during Ocean Drilling

Program Leg 155 (Sites 945 and 946; see supplementary Fig. S1), which are proximal to one another and easily correlated (see Flood et al., 1995; Mason et al., 2019). We amalgamate these subsamples (See supplemental Fig. S1) to better characterize complex thermotectonic histories of sediment from the Amazon Fan. This approach integrates sedimentation on the Amazon Fan over multi-millennial timescales (MIS-6 through MIS-2; ~180 – 20 ka; Flood et al., 1995).

Results

4.1 Detrital Zircon U-Pb and U-Th/He Double Dating

U-Pb and ZHe ages from 114 DZs recovered from the Amazon Fan characterize the thermotectonic histories experienced by DZs in the Amazon system. Complete isotopic measurements may be found in Supplementary datafile S1. Figure 2 displays a cross plot of ZHe age vs. U-Pb age, with associated kernel density estimates (KDEs) and histograms. Figure 3 A – D displays cross plots of select U-Pb age groups (0 – 200 Ma, 200 – 400 Ma, 400 – 900 Ma, and 900 – 1300 Ma). Only two individual DZs resulted in ZHe ages greater than their associated U-Pb ages (Fig. 2), and are thus excluded from further analyses. In the following paragraphs, we report the resultant proportions of ZHe cooling ages, and relate these ZHe ages to their associated U-Pb age populations.

4.2 First Cycle Volcanic Zircons

Six first cycle volcanic DZs were identified by their overlapping U-Pb and ZHe ages (within analytical error; Campbell et al., 2005; Saylor et al., 2012). These first cycle volcanic DZs range in age from ~30 Ma – 585 Ma, with the majority (four of six) from Mesozoic and Cenozoic U-Pb age groups (Fig 3 A). Of the five DZs with Cenozoic U-Pb ages, only two have errors that overlap, and are first cycle volcanic zircons (*sensu stricto*). The remaining three Cenozoic DZs have ZHe ages that are several Myr younger (~3 – 10 Myr) than their associated U-Pb ages.

4.3 U-Th/He Age Groups

Of the 112 accepted ZHe ages, 38% (n=42/112) are Cenozoic, 22% (n=25/112) are Mesozoic, 29% (n=32/112) are Paleozoic, and 12% (n=13/112) are Precambrian in age (Fig. 2). ZHe age density increase dramatically across the Ediacaran (< ~600 Ma) and through the Phanerozoic, while very few DZs record cooling older than the beginning of the Pan African-Brasiliano orogeny (> ~900 Ma). We document important ZHe age modes (or populations) present in the dataset, from old to young (see also Fig. 2): (1) an Ediacaran mode (~575 – 600 Ma), (2) a distributed late Cambrian through early Carboniferous mode (~500 – 350 Ma), (3) a latest Carboniferous to middle Permian mode (~300 – 275 Ma), (4) a late Triassic to Early Jurassic mode (~225 – 175 Ma), (5) a minor Early Cretaceous mode (~110 – 125), (6) a late Cretaceous through Paleocene mode (~75 – 50 Ma), and finally (7) a Miocene through recent mode (25 –

0 Ma). The most prominent population of ZHe ages falls in the middle – late Miocene, with a peak mode at ~12 Ma (Fig 2).

4.4 ZHe Ages in Context of U-Pb Age Populations

Relationships between DZ U-Pb and ZHe ages yield insights into the functioning of sediment routing systems and thermal histories experienced by their sediment loads. In the Amazon Fan, the majority of DZs with U-Pb ages >1300 Ma, often interpreted as cratonic DZs, display distributed ZHe cooling ages across the Late Neoproterozoic, Paleozoic, and middle Mesozoic (Fig. 2). However, several early – late Cenozoic ZHe ages occur in this oldest U-Pb age group, and record recent cooling for at least some proportion of age groups normally interpreted as craton derived.

A large proportion of DZs present in the Amazon Fan have U-Pb ages that correspond to the Sunsás orogeny (~29%; Mason et al., 2019; this study 24%; *n* = 27/112), yet only two ZHe ages record cooling associated with that period of time (900 – 1300 Ma). Instead, the Sunsás U-Pb age group is associated with ZHe cooling ages between ~200 – 600 Ma, and a distinct mode of late Cretaceous through Neogene ZHe ages, (n=12/27; ~5 – 72 Ma; Fig. 3 D), with the majority of youngest ZHe ages recording cooling during the late Miocene.

DZs with U-Pb ages between 400 – 900 Ma (28% of DZs in this study; Fig. 3 C) are typically attributed to terranes that record orogenesis during the Pan African – Brasiliano orogenies (550 – 900 Ma), and the Cambro-Orovician Pampean – Famatinian orogenies. This U-Pb age group contains ZHe age modes at ~400 – 550 Ma, ~250 – 300 Ma, ~200 Ma, and a diffuse population of Early Cretaceous through Paleogene ZHe ages, but lacks Neogene ZHe ages.

DZs with U-Pb ages between 200 – 400 Ma (15% of DZs in this study; Fig. 3 B) are likely associated with magmatism during Gondwanan orogenesis across the Carboniferous through Permian, with magmatism of equivalent age to Permo-Triassic Choiyoi volcanism, and with arc magmatism along the SW margin of Gondwana from the late Triassic through the early Jurassic. Devonian and Carboniferous U-Pb ages are associated with Cenozoic and late Cretaceous ZHe ages, respectively (Fig. 3 B). Permo-Triassic U-Pb ages are associated with one first cycle volcanic zircon, sparse late Triassic to early Cretaceous ZHe ages, and a high proportion of Cenozoic ZHe cooling ages. Overall, this U-Pb age group is dominated by Cenozoic ZHe ages.

Those DZs with U-Pb ages between 0 – 200 Ma (Fig 3 A) have a significant component of first cycle volcanic zircons, or are associated largely with late Cenozoic cooling ages (<50 Ma). Jurassic and early Cretaceous U-Pb ages are associated with one first cycle volcanic, and many Neogene ZHe ages. DZs with late Cretaceous or younger U-Pb ages are first cycle volcanic, or associated with Paleogene through Neogene ZHe ages.

4.5 Synthesis of Detrital Age Data From the Amazon Fan

DZs sampled from the Amazon Fan integrate sedimentation across >150 kyr of the late Pleistocene glacial times, and taps into erosional sources across the Amazon Basin, with most sediment coming from the high elevation Andean streams. Through the relationships of U-Pb provenance and ZHe ages, we can begin to understand the thermal histories of distinct DZ source terranes.

Late Mesoproterozoic through Cambro-Ordovician U-Pb DZ age groups display several ZHe age modes that broadly record cooling during the early Paleozoic, the Permian, the Late Triassic – Early Jurassic, and the Late Cretaceous – Neogene (Fig 3). The Proterozoic (900 – 1300 Ma) Sunsás U-Pb age group, much like the 400 – 900 Ma U-Pb age group, broadly records cooling across the Phanerozoic, but has an additional component of Neogene ZHe ages.

The 200 – 400 Ma U-Pb age group records cooling events in the Late Triassic – Early Jurassic, the Cretaceous, and the Cenozoic. The youngest U-Pb age group, 200 – 0 Ma, contains Jurassic and Cretaceous DZs that cooled in the Neogene, in the Cretaceous, and several Cenozoic first-cycle volcanics. Jurassic and Cretaceous DZs share a history of recent cooling with each of the other U-Pb age groups.

There are several temporal gaps, or lulls, in cooling of crustal material in our dataset. For example, the period between the Late Jurassic through Early Cretaceous (Fig 3) lacks ZHe ages, save for three Late Cretaceous ZHe ages associated with Pan African-Brasiliano aged DZs (~700 – 900 Ma). Other significant lulls in crustal cooling occur between ~75 – 100 Ma, ~225 – 250 Ma, and from ~325 – 375 Ma, as displayed in the ZHe KDE on the vertical axis of Figure 2.

Collectively, DZs from the Amazon Fan record cycles of magmatism and crustal cooling during the Phanerozoic, with the density of ZHe age data increasing through the late Miocene. This dataset of thermal information provides a unique opportunity to integrate and analyze cyclicity of magmatic and crustal cooling events for much of the Central and Northern Andes.

4.6 Frequency Analysis of ZHe Age Data

In order to quantitatively evaluate the periodicity of hypothesized cyclic orogenic processes (e.g., DeCelles et al., 2015; Sundell et al., 2019a) we analyzed the KDE interval between 650-40 Ma of the ZHe record (Fig. 4). By excluding the last 40 Ma of the record we aimed to avoid distortion of the spectrum, given the significant increase in the data over that portion of the record (Weedon, 2003). To estimate the spectral characteristics of the record we used the R package *Astrochron* (Meyers, 2014) to carry out power spectra analysis using the Mann and Lees (1996) robust red noise Multi-Taper method (MTM) analysis to test for statistical significance of spectral peaks. Prior to analysis the KDE was interpolated to even sample spacing, prewritten using an autoregressive-1 (AR1) filter, and detrended. We report periodicities that exceed the 85% and 90% MTM harmonic F-test confidence level estimate, while also achieving the required robust red noise confidence level (85%) within +/- half the power spectrum bandwidth resolution.

This method of estimation substantially reduces the identification of false positive estimates of spectra peaks (Meyers, 2012). The results of the frequency analysis (Fig. 4) show statistically significant periodicity in cooling age frequency that occur at 57 and 92 Myr periods (>90% and 85% confidence level, respectively).

Discussion

5.1 Provenance of Amazon Fan Sediment

The distribution of DZ U-Pb and U-Th/He double dates from sediment of the Amazon Fan is representative of clastic detritus transferred from the Amazon River to the Atlantic Ocean over late Pleistocene timescales (Fig. 5). All U-Pb crystallization age groups from the fan have some component of recent cooling ages, suggesting tectonic exhumation in the Andes. New DZ double dates support previous interpretations; the majority of the Amazon Fan DZs are derived from the central and northern Andes (Mason et al., 2019), rather than the more areally extensive but low relief Amazon craton. Indeed, while the Andes represent a relatively small fraction (areally) of the Amazon drainage basin (~12%), the Cordilleran system contributes a disproportionate amount of DZs with Cenozoic ZHe cooling ages (38% of total) to the Amazon Fan. DZs with U-Pb ages <400 Ma are likely sourced entirely from the Andes (Fig. 3 A & B), as most DZs in this U-Pb age group are either first cycle volcanic zircons, have Triassic – Jurassic ZHe ages, or have late Cretaceous through Neogene ZHe ages. Although DZs with Andean arc U-Pb ages (*sensu stricto*; 0 – 50 Ma) are scarce (n = 4/112), ZHe cooling ages display the most pronounced mode between 0 – 50 Ma (Fig. 2), demonstrating the importance of tectonic driven erosion of the Cordillera to the ultimate transfer of sediment to the Atlantic margin. This interpretation is consistent with relatively high rates of denudation measured using ^{10}Be in modern Andean sourced streams (Wittmann et al. 2011).

Craton aged DZs (>1300 Ma) correspond largely to Neoproterozoic and Paleozoic ZHe cooling ages, which could be interpreted as sediment recycling in the cordillera or primary cratonic sources. Exhumation between 400 – 500 Ma involved uplift and erosion of Sunsás (900 – 1300 Ma) through early Paleozoic aged rocks, as shown by the U-Pb and ZHe relationships of DZs (Fig. 2; Fig. 3D & 3C). The mode of ZHe cooling ages between ~400 – 500 Ma are consistent with a documented long-lived, and spatially continuous active margin (the Famatinian orogeny) along western Gondwana that was roughly contemporaneous with the Taconic orogeny of Laurentia (Chew et al., 2007). Although Neoproterozoic through craton aged DZs are documented in Andean rivers (Capaldi et al., 2017; Jackson et al., 2019), Cenozoic cooling ages associated with those U-Pb age groups provides another line of evidence that recycling (sedimentation, burial heating, and later exhumation) of older cratonic DZs is common in the Cordillera of South America.

5.2 Past Cycles of Orogenesis Preserved in the Amazon Fan

Our frequency analysis of ZHe age data suggests an unrecognized periodicity in crustal cooling events archived in the Amazon Fan, which we interpret to be related to the history of upper and lower plate coupling along the subduction dominated western margin of South America. The existence of distinct modes of ZHe cooling ages (Fig. 4), separated by periods of apparently low rates of cooling, suggests episodic thermotectonic events recorded by Amazon Fan detritus. Furthermore, distinct modes of ZHe cooling ages partially overlap, precede, or temporally lag modes of U-Pb ages, suggesting a potential causal relationship between magmatic flux events (modes of U-Pb ages), and crustal cooling (ZHe age modes; Fig. 4 A, B).

The conceptual model suggested by DeCelles et al. (2015) explicitly predicts the creation of orogenic relief, associated with underthrusting of melt fertile crust, and isostatic surface uplift in response to delamination of dense lithospheric mantle beneath the orogen. Before or during the waning phase of a high flux magmatic event, the width of the orogen may grow as the fold-thrust belt propagates, allowing for enhanced exhumation and cooling of material along thrust sheets or from exhumed sedimentary basins. Carrapa and Decelles (2015) interpreted an anticorrelation between magmatic flux, deformation of the orogen, and crustal cooling, to suggest deformation temporally proceeds magmatic flux. Our dataset also suggests that magmatic flux and exhumational cooling are linked for the portions of the Andes sampled by the Amazon River. The timescales of these processes, as delineated by our spectral analysis of ZHe age data, are roughly 57 Ma and 92 Ma, consistent with prior estimates (25 – 50 Myr; DeCelles et al., 2015; ~70 Myr; Sundell et al, 2019a; Sundell et al., 2019b). Figure 6 examines the recent (0 – 200 Ma) relationship between magmatic flux events and crustal cooling recorded by the Amazon Fan, and further highlights an apparent temporal relationship between magmatic events and subsequent punctuated crustal cooling.

The Amazon Fan is a high resolution archive for past cycles of orogeneisis. for example, Figure 6 displayes the recent 200 Ma history, and highlights a Paleogene increase in ZHe age density, followed by a minor lull at ~40 Ma, and a subsequent major Neogene increase, a pattern which coincides well with widely identified inception of coarse grained sedimentation in the Late Cretaceous and Paleogene, followed by an Eocene-Oligocene hiatus, and finally resumed coarse grained sedimentation in retroact foreland basins during the along strike of the Andes (Horton, 2018a).

Here we suggest that cyclic orogenic phenomena proposed for Andean style mountain building (DeCelles et al., 2009; DeCelles et al., 2015; Sundell et al., 2019) may result in a causal temporal relationship between high magmatic flux events, and pulsed crustal cooling (Fig. 6). For example, Jurassic through Neogene orogenesis is well documented during the formation of the modern Andes (Garzione et al., 2008; Horton, 2018); ZHe ages from the Amazon Fan record cycles of magmatism and increased crustal cooling during the Jurassic (~180 Ma), Cretaceous (~110 Ma) and latest Cretaceous – early Paleogene (~60-70 Ma), and early late Miocene (~12 Ma), which are consistent with a cyclic pace of orogenesis proposed for the central to northern Andes (DeCelles et al., 2015; Sundell et al., 2018; 2019a).

We hypothesize numerous exhumational cooling events remain recorded in the ZHe cooling ages of upland Andean bedrock areas of the eastern Cordillera (see Reiners et al., 2015), for example in the extensive Paleozoic metamorphic and siliciclastic units exposed in the eastern Andes of Bolivia and Peru (Gomez Tapias et al., 2019). This would explain the abundance of Paleozoic ZHe cooling ages found in what is hypothesized to be largely Andean derived clastic sediment from the northern central and northern Andes.

Others have interpreted distinct age populations of large detrital ZHe data sets in terms of regional tectonic histories; for instance, in the Columbian foreland basin sedimentary formations of Cretaceous through Neogene ages yield ZHe age populations that are interpreted to correlate to Cenozoic Andean exhumation, Cretaceous rifting/unroofing, assembly of Gondwana (Gondwanide orogeny), and the Famatinian orogeny (Odoh et al., 2019). Here, ZHe cooling ages from the Amazon Fan—a reliable repository of the entire continent-scale catchment—can be viewed as a detrital record of as many as six distinct phases of exhumation driven cooling along western Gondwana – western South American margin since the late Neoproterozoic (Figs. 5 & 6).

Conclusions

The Amazon Fan, offshore NE South America, preserves a record of sediment transfer largely from the Andes of western South America. New detrital zircon (DZs) U-Pb and U-Th/He (ZHe) double dating from the late Pleistocene Amazon Fan (MIS-6 – MIS-2) confirm the efficient sediment transfer (from greater than 3000 km) from Andean hinterlands to the deep-sea over multi-millennial timescales. Though U-Pb DZ ages alone may yield ambiguous provenance, approximately 40% of DZs measured have Cenozoic ZHe cooling ages, demonstrating the importance of exhumational cooling in the active cordillera on sediment sourcing to the passive margin. Andean detritus preserves a deep-time thermotectonic record of periodic thermal events, which we interpret as subduction related orogenesis, and resulting cooling of crustal material, beginning with the assembly of Gondwana during the late Neoproterozoic (~600 Ma), through uplift and deformation of the modern Andes in the late Miocene. Spectral analysis, applied to the ZHe data set, suggests an unrecognized cyclicity in thermal events taking place in the central and northern Andes (over ~57 and ~92 Ma periods) preserved in the ZHe cooling ages from the Amazon Fan. We hypothesize this is the thermotectonic signal of recurring geodynamic processes that led to high fluxes of magma to the arc, associated with relief construction and subsequent destruction along the active western margin of South America.

Declarations

Acknowledgements

The authors wish to acknowledge Equinor for grant funding.

Author Contributions

CM, BWR, AF, and DFS contributed to the design of the study. MP and CM coordinated and performed the frequency analysis of ZHe age data. All authors contributed to the writing of the manuscript.

References

Armijo, R., Lacassin, R., Coudurier-Curveur, A., & Carrizo, D. (2015). Coupled tectonic evolution of Andean orogeny and global climate. In *Earth-Science Reviews* (Vol. 143, pp. 1–35). Elsevier. https://doi.org/10.1016/j.earscirev.2015.01.005

Bernal, I., Tavera, H., and Antayhua, Y., (2002). Zonas sismogenica en el Peru: volumenes de informacion, graficos polares y zonificacion preliminary: Sociedad Geologica de Peru, Boletin, v. 93, p. 31–44.

Blum, M., Rogers, K., Gleason, J., Najman, Y., Cruz, J., & Fox, L. (2018). Allogenic and Autogenic Signals in the Stratigraphic Record of the Deep-Sea Bengal Fan. *Scientific Reports*, *8*(1). https://doi.org/10.1038/s41598-018-25819-5

Campbell, I. H., Reiners, P. W., Allen, C. M., Nicolescu, S., & Upadhyay, R. (2005). He-Pb double dating of detrital zircons from the Ganges and Indus Rivers: Implication for quantifying sediment recycling and provenance studies. *Earth and Planetary Science Letters*, *237*(3–4), 402–432. https://doi.org/10.1016/j.epsl.2005.06.043

Capaldi, T. N., Horton, B. K., McKenzie, N. R., Stockli, D. F., & Odlum, M. L. (2017). Sediment provenance in contractional orogens: The detrital zircon record from modern rivers in the Andean fold-thrust belt and foreland basin of western Argentina. *Earth and Planetary Science Letters*, *479*, 83–97. https://doi.org/10.1016/j.epsl.2017.09.001

Carrapa, B., & DeCelles, P. G. (2015). Regional exhumation and kinematic history of the central Andes in response to cyclical orogenic processes. In P. G. DeCelles, M. N. Ducea, B. Carrapa, & P. A. Kapp (Eds.), *Geodynamics of a Cordilleran Orogenic System: The Central Andes of Argentina and Northern Chile* (Vol. 212, p. 0). Geological Society of America. https://doi.org/10.1130/2015.1212(11)

Chen, YW., Wu, J. & Suppe, J. Southward propagation of Nazca subduction along the Andes. *Nature* **565,** 441–447 (2019). https://doi.org/10.1038/s41586-018-0860-1

Chew, D. M., Cardona, A., & Mišković, A. (2011). Tectonic evolution of western Amazonia from the assembly of Rodinia to its break-up. *International Geology Review*, *53*(11–12), 1280–1296. https://doi.org/10.1080/00206814.2010.527630

Chew, D. M., Pedemonte, G., & Corbett, E. (2016). Proto-Andean evolution of the Eastern Cordillera of Peru. *Gondwana Research*, *35*, 59–78. https://doi.org/10.1016/j.gr.2016.03.016

Decelles, P. G., Ducea, M. N., Kapp, P., & Zandt, G. (2009). Cyclicity in Cordilleran orogenic systems. In *Nature Geoscience* (Vol. 2, Issue 4, pp. 251–257). https://doi.org/10.1038/ngeo469

DeCelles, P. G., Zandt, G., Beck, S. L., Currie, C. A., Ducea, M. N., Kapp, P., Gehrels, G. E., Carrapa, B., Quade, J., & Schoenbohm, L. M. (2015). Cyclical orogenic processes in the Cenozoic central Andes. *Memoir of the Geological Society of America*, *212*, 459–490. https://doi.org/10.1130/2015.1212(22)

Fildani, A., Hessler, A. M., Mason, C. C., McKay, M. P., & Stockli, D. F. (2018). Late Pleistocene glacial transitions in North America altered major river drainages, as revealed by deep-sea sediment. *Scientific Reports*, *8*(1). https://doi.org/10.1038/s41598-018-32268-7

Fildani, A., McKay, M. P., Stockli, D., Clark, J., Dykstra, M. L., Stockli, L., & Hessler, A. M. (2016). The ancestral Mississippi drainage archived in the late Wisconsin Mississippi deep-sea fan. *Geology*, *44*(6), 479–482. https://doi.org/10.1130/G37657.1

Flood, R.D., Piper, D.J.W., Klaus, A., et al., 1995. Proceedings of the Ocean Drilling Program, Initial Reports, Volume 155: College Station, Texas, Ocean Drilling Program, https://doi.org/10.2973/odp.proc.ir.155.1995.

Fosdick, J. C., Grove, M., Graham, S. A., Hourigan, J. K., Lovera, O., & Romans, B. W. (2015). Detrital thermochronologic record of burial heating and sediment recycling in the Magallanes foreland basin, Patagonian Andes. *Basin Research*, *27*(4), 546–572. https://doi.org/10.1111/bre.12088

Garzione, C. N., Hoke, G. D., Libarkin, J. C., Withers, S., Macfadden, B., Eiler, J., Ghosh, P., & Mulch, A. (2008). Rise of the Andes. 10.1126/science.1148615

Garzione, C. N., Hoke, G. D., Libarkin, J. C., Withers, S., Macfadden, B., Eiler, J., Ghosh, P., & Mulch, A. (2008). *Rise of the Andes*. www.sciencemag.org

George, S. W. M., Horton, B. K., Jackson, L. J., Moreno, F., Carlotto, V., & Garzione, C. N. (2019). Sediment provenance variations during contrasting Mesozoic-early Cenozoic tectonic regimes of the northern Peruvian Andes and Santiago-Marañón foreland basin. In *Andean Tectonics* (pp. 269–296). Elsevier. https://doi.org/10.1016/b978-0-12-816009-1.00012-5

Gibbs, R. J. Geochemistry of the Amazon system part 1. (1967). *Geological Society of America Bulletin*, *78*, 1203–1232.

Hart, N. R., D. F. Stockli, and N. W. Hayman (2016), Provenance evolution during progressive rifting and hyperextension using bedrock and detrital zircon U-Pb geochronology, Mauléon Basin, western Pyrenees, Geosphere, 12(4), 1166–1186.

Hessler, a. M., & Fildani, a. (2015). Andean Forearc Dynamics, As Recorded By Detrital Zircon From the Eocene Talara Basin, Northwest Peru. *Journal of Sedimentary Research*, *85*(6), 646–659. https://doi.org/10.2110/jsr.2015.45

Hessler, A. M., & Fildani, A. (2019). Deep-sea fans: tapping into Earth's changing landscapes. *Journal of Sedimentary Research*, *89*(11), 1171–1179. https://doi.org/10.2110/jsr.2019.64

Hoorn, C., Bogotá-A, G. R., Romero-Baez, M., Lammertsma, E. I., Flantua, S. G. A., Dantas, E. L., Dino, R., do Carmo, D. A., & Chemale, F. (2017). The Amazon at sea: Onset and stages of the Amazon River from a marine record, with special reference to Neogene plant turnover in the drainage basin. *Global and Planetary Change*, *153*, 51–65. https://doi.org/10.1016/j.gloplacha.2017.02.005

Horton, B. K. (2018a). Sedimentary record of Andean mountain building. *Earth-Science Reviews*, *178*(March), 279–309. https://doi.org/10.1016/j.earscirev.2017.11.025

Horton, B. K. (2018b). Tectonic Regimes of the Central and Southern Andes: Responses to Variations in Plate Coupling During Subduction. *Tectonics*, *37*(2), 402–429. https://doi.org/10.1002/2017TC004624

Horton, B. K., Anderson, V. J., Caballero, V., Saylor, J. E., Nie, J., Parra, M., & Mora, A. (2015). Application of detrital zircon U-Pb geochronology to surface and subsurface correlations of provenance, paleodrainage, and tectonics of the Middle Magdalena Valley Basin of Colombia. *Geosphere*, *11*(6), 1790–1811. https://doi.org/10.1130/GES01251.1

Jackson, L. J., Horton, B. K., & Vallejo, C. (2019). Detrital zircon U-Pb geochronology of modern Andean rivers in Ecuador: Fingerprinting tectonic provinces and assessing downstream propagation of provenance signals. *Geosphere*, *15*(6), 1943–1957. https://doi.org/10.1130/GES02126.1

Jorge Gómez Tapias, Carlos Schobbenhaus, & Nohora Emma Montes Ramírez. (2019). *Geologic Map of South America at a Scale of 1:5 M*.

Kontak, D.J., Clark, A.H., Farrar, E., Archibald, D.A., Baadsgaard, H., 1990. Late Paleozoic-early Mesozoic magmatism in the Cordillera de Carabaya, Puno, southeastern Peru: Geochronology and petrochemistry. J. S. Am. Earth Sci. 3 (4), 213–230.

Mann, M. E., & Lees, J. M. (1996). Robust estimation of background noise and signal detection in climatic time series. *Climatic Change*, *33*(3), 409–445. https://doi.org/10.1007/BF00142586

Maslin, M. (2009). Review of the Timing and Causes of the Amazon-Fan Mass Transport and Avulsion Deposits During the Latest Pleistocene. *External Controls on Deep-Water Depositional Systems*, *92*(92), 133–144. https://doi.org/10.2110/sepmsp.092

Mason, C. C., Fildani, A., Gerber, T., Blum, M. D., Clark, J. D., & Dykstra, M. (2017). Climatic and anthropogenic influences on sediment mixing in the Mississippi source-to-sink system using detrital zircons: Late Pleistocene to recent. *Earth and Planetary Science Letters*, *466*, 70–79. https://doi.org/10.1016/j.epsl.2017.03.001

Mason, C. C., Romans, B. W., Stockli, D. F., Mapes, R. W., & Fildani, A. (2019). Detrital zircons reveal sea-level and hydroclimate controls on Amazon River to deep-sea fan sediment transfer.

Geology. https://doi.org/10.1130/G45852.1

McDaniel, D.K., McLennan, S.M., and Hanson, G.N., 1997, Provenance of the Amazon Fan muds: Constraints from Nd and Pb isotopes, in Flood, R.D., Piper, D.J.W., Klaus, A., and Peterson, L.C., eds., Proceedings of the Ocean Drilling Program, Scientific Results: College Station, Texas, Ocean Drilling Program, v. 155, p.169–176.

McQuarrie, N., Barnes, J. B., & Ehlers, T. A. (2008). Geometric, kinematic, and erosional history of the central Andean Plateau, Bolivia (15-17°S). *Tectonics*, *27*(3). https://doi.org/10.1029/2006TC002054

Meade, R. H., Nordin, C. F., Curtis, W. F., Costa Rodrigues, F. M., do Vale, C. M., & Edmond, J. M. (1979). Sediment loads in the Amazon River. *Nature,* 278, 161–163). https://doi.org/10.1038/278161a0

Meyers, S. R. (2012). Seeing red in cyclic stratigraphy: Spectral noise estimation for astrochronology. *Paleoceanography*, *27*(3). https://doi.org/10.1029/2012PA002307

Meyers, S. R. (2014). *Astrochron: An R package for astrochronology*.

Milliman, J.D., and Farnsworth, K.L., (2011). River Discharge to the Coastal Ocean: A Global Synthesis: Cambridge, UK, Cambridge University Press, 384 p., https://doi.org/10.1017/CBO9780511781247.

Odlum, M. L., Stockli, D. F., Capaldi, T. N., Thomson, K. D., Clark, J., Puigdefàbregas, C., & Fildani, A. (2019). Tectonic and sediment provenance evolution of the South Eastern Pyrenean foreland basins during rift margin inversion and orogenic uplift. *Tectonophysics*, *765*, 226–248. https://doi.org/10.1016/j.tecto.2019.05.008

Odoh, S., Saylor, J. E., Higuera, C., Copeland, P., & Lapen, T. J. (2019). Discriminating mechanisms for coarse clastic progradation in the Colombian foreland basin using detrital zircon double dating. In *Andean Tectonics* (pp. 133–171). Elsevier. https://doi.org/10.1016/b978-0-12-816009-1.00008-3

Paterson, S. R., & Ducea, M. N. (2015). Arc magmatic tempos: Gathering the evidence. *Elements*, *11*(2), 91–98. https://doi.org/10.2113/gselements.11.2.91

Pepper, M., Gehrels, G., Pullen, A., Ibanez-mejia, M., Ward, K. M., & Kapp, P. (2016). *Magmatic history and crustal genesis of western South America : Constraints from U-Pb ages and Hf isotopes of detrital zircons in modern rivers*. *12*(5), 1532–1555. https://doi.org/10.1130/GES01315.1

Ramos, V. A. (2018). *The Famatinian Orogen Along the Protomargin of Western Gondwana: Evidence for a Nearly Continuous Ordovician Magmatic Arc Between Venezuela and Argentina* (pp. 133–161). https://doi.org/10.1007/978-3-319-67774-3_6

Reiners, P. W. (2005). Zircon (U-Th)/He Thermochronometry. *Reviews in Mineralogy and Geochemistry*, *58*(1), 151–179. https://doi.org/10.2138/rmg.2005.58.6

Reiners, P. W., & Brandon, M. T. (2006). Using thermochronology to understand orogenic erosion. *Annual Review of Earth and Planetary Sciences*, *34*, 419–466. https://doi.org/10.1146/annurev.earth.34.031405.125202

Reiners, P. W., Thomson, S. N., Vernon, A., Willett, S. D., Zattin, M., Einhorn, J., Gehrels, G., Quade, J., Pearson, D., Murray, K. E., & Cavazza, W. (2015). Low-temperature thermochronologic trends across the central Andes, 21°S-28°S. *Memoir of the Geological Society of America*, *212*, 215–249. https://doi.org/10.1130/2015.1212(12)

Schwartz, T. M., Schwartz, R. K., & Weislogel, A. L. (2019). Orogenic Recycling of Detrital Zircons Characterizes Age Distributions of North American Cordilleran Strata. *Tectonics*, *38*(12), 4320–4334. https://doi.org/10.1029/2019TC005810

Sundell, K. E., Saylor, J. E., Lapen, T. J., & Horton, B. K. (2019b). Implications of variable late Cenozoic surface uplift across the Peruvian central Andes. *Scientific Reports*, *9*(1). https://doi.org/10.1038/s41598-019-41257-3

Sundell, K., Saylor, J. E., & Pecha, M. (2019a). Provenance and recycling of detrital zircons from Cenozoic Altiplano strata and the crustal evolution of western South America from combined U-Pb and Lu-Hf isotopic analysis. In *Andean Tectonics* (pp. 363–397). Elsevier. https://doi.org/10.1016/b978-0-12-816009-1.00014-9

Thomson, K. D., Stockli, D. F., Clark, J. D., Puigdefàbregas, C., & Fildani, A. (2017). Detrital zircon (U-Th)/(He-Pb) double-dating constraints on provenance and foreland basin evolution of the Ainsa Basin, south-central Pyrenees, Spain. *Tectonics*, *36*(7), 1352–1375. https://doi.org/10.1002/2017TC004504

van der Lelij, R., Spikings, R., Ulianov, A., Chiaradia, M., & Mora, A. (2016). Paleozoic to Early Jurassic history of the northwestern corner of Gondwana, and implications for the evolution of the Iapetus, Rheic and Pacific Oceans. *Gondwana Research*, *31*, 271–294. https://doi.org/10.1016/j.gr.2015.01.011

Weedon, G. P. (2003). *Time-Series Analysis and Cyclostratigraphy: Examining Stratigraphic Records of Environmental Cycles*. Cambridge: Cambridge University Press. https://doi.org/10.1017/CBO9780511535482

Wittmann, H., von Blanckenburg, F., Maurice, L., Guyot, J. L., Filizola, N., & Kubik, P. W. (2011). Sediment production and delivery in the Amazon River basin quantified by in situ-produced cosmogenic nuclides and recent river loads. *Bulletin of the Geological Society of America*, *123*(5), 934–950. https://doi.org/10.1130/B30317.1

Wolfe, M. R., and D. F. Stockli (2010), Zircon (U–Th)/He thermochronometry in the KTB drill hole, Germany, and its implications for bulk He diffusion kinetics in zircon, Earth Planet. Sci. Lett., 295(1), 69–82.

Figures

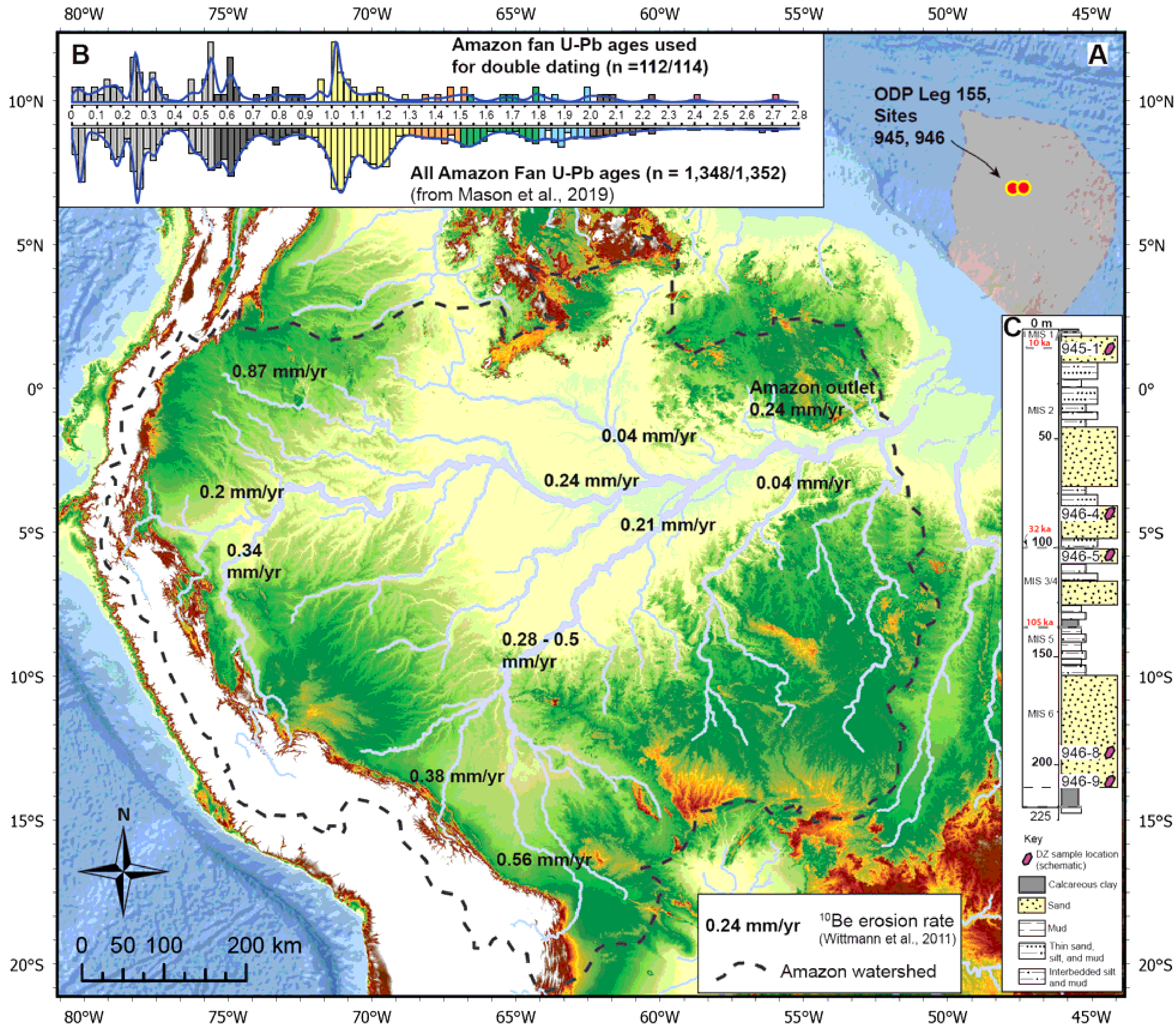

Figure 1

A: Elevation map of the Amazon drainage basin and approximate extents of the Amazon deep-sea fan. Tributaries and main-stem Amazon River presented with 10Be-derived erosion rates (Wittmann et al., 2011). B: Detrital zircon U-Pb ages from the Amazon fan used in this study, and those from Mason et al., 2019. C: Composite lithostratigraphy from ODP Leg 155, sites 945 and 946 with schematic detrital zircon sample locations (after Mason et al., 2019).

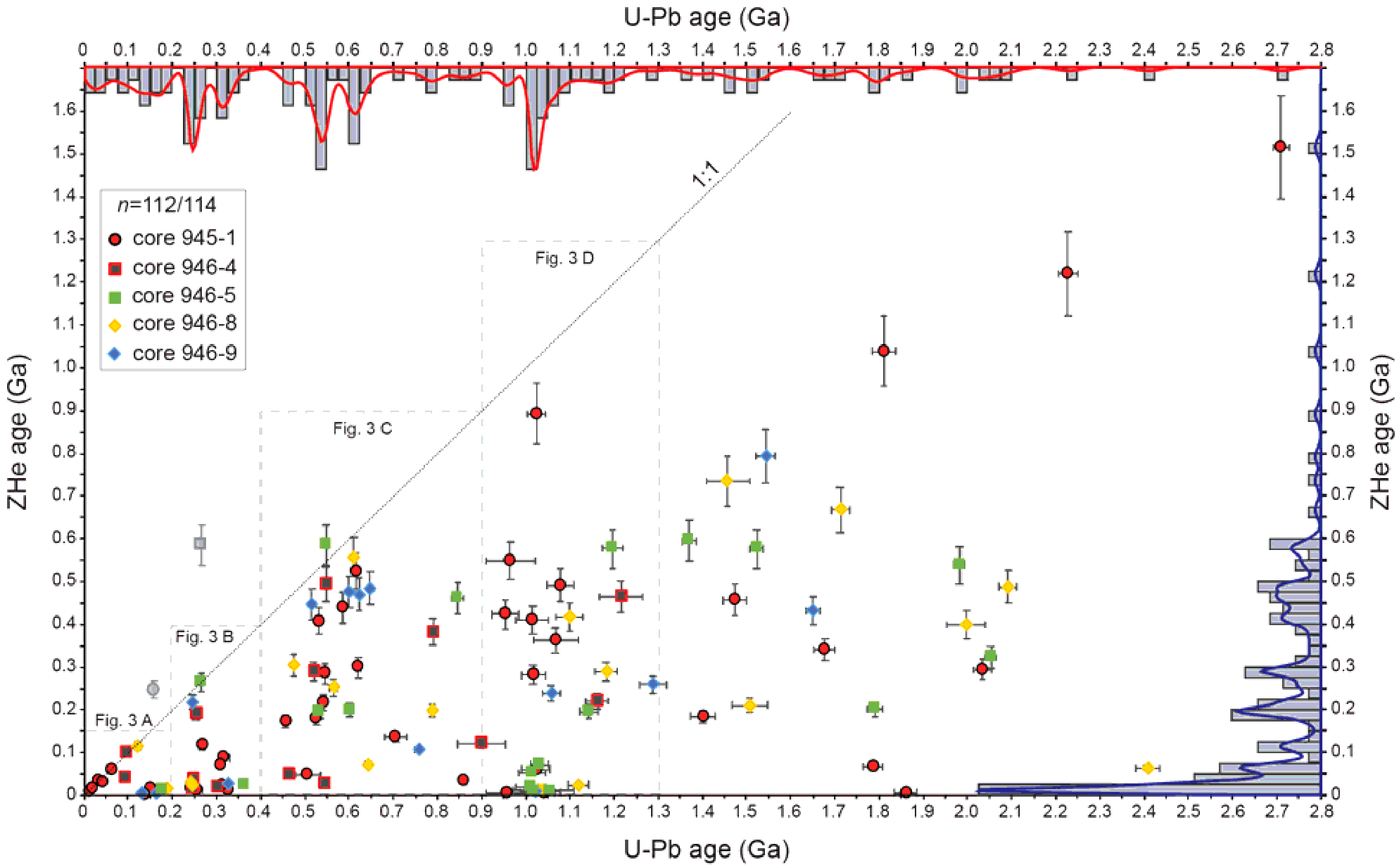

Figure 2

Cross plot and kernel density estimates of U-Pb and U-Th/He double dates from detrital zircons recover from the late Pleistocene Amazon fan (Leg 155, Sites 945, 946). Age bins at 25 Ma increments. See Supplementary Figure S1 for individual sample data from cores 945-1 and 946.

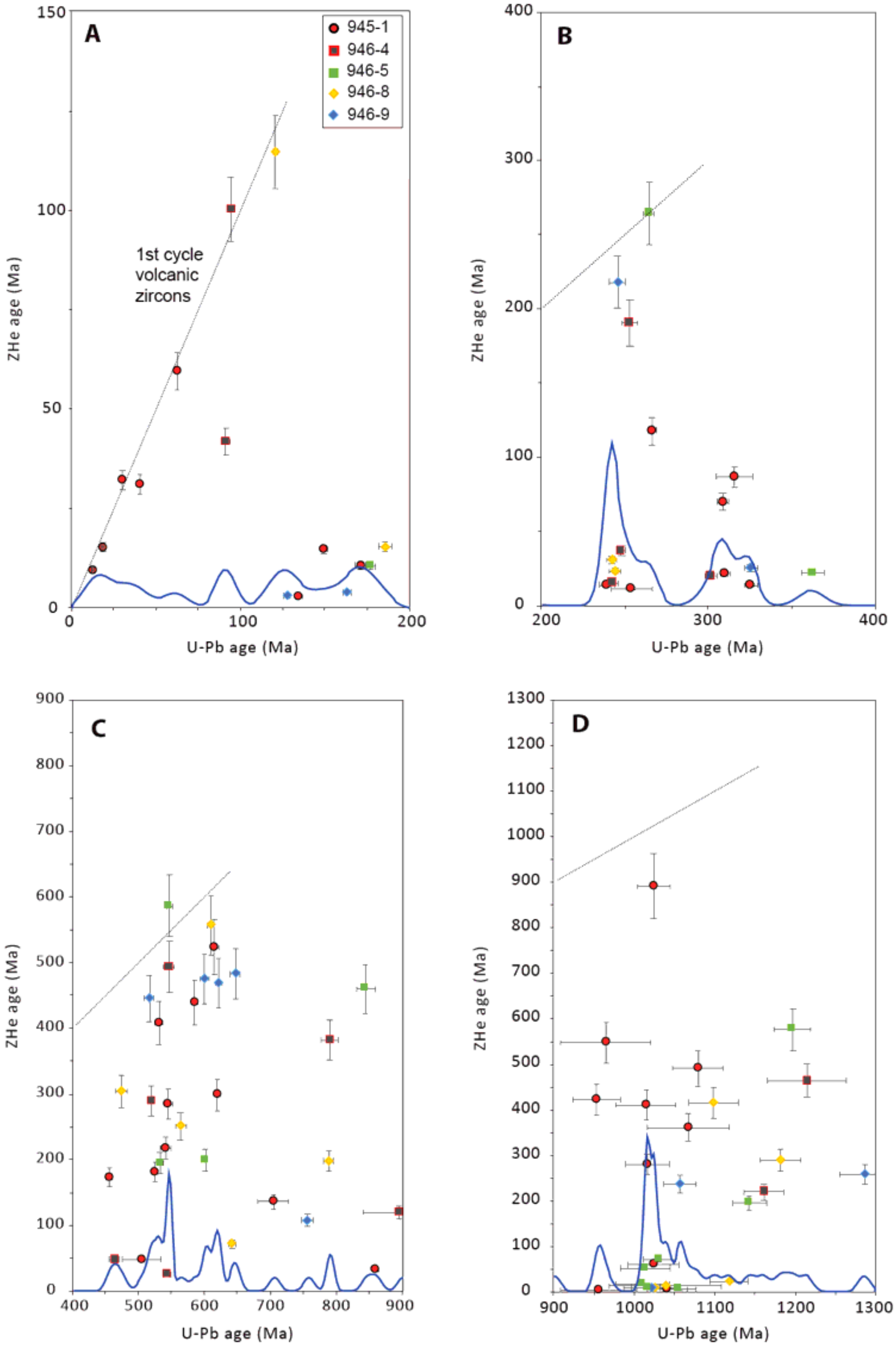

Figure 3

Cross plots for detrital zircon U-Pb and U-Th/He double dates, organized by U-Pb age group: A: 0 – 200 Ma, B: 200 – 400 Ma, C: 400 – 900 Ma, and D: 900 – 1300 Ma. Kernel density estimates represents the U-Pb age density for each group. Note scale changes across A-C.

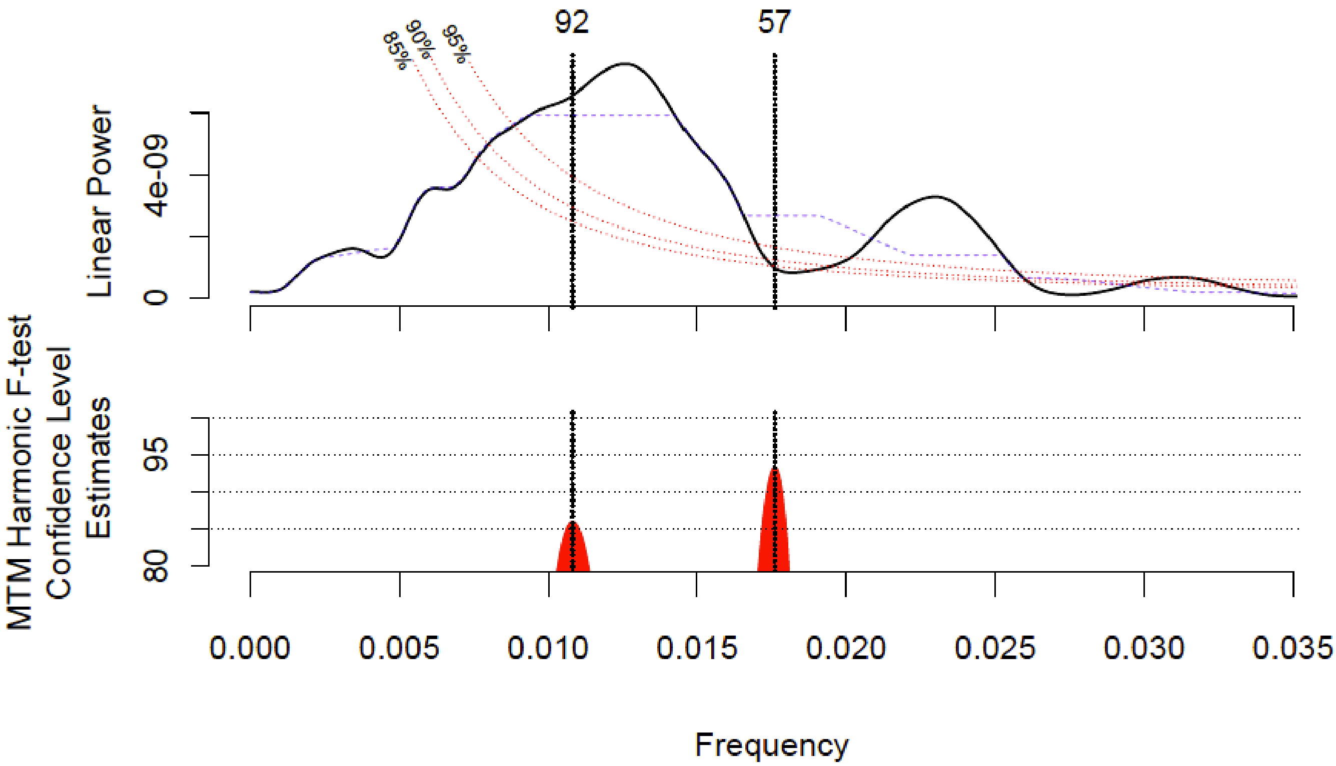

Figure 4

Spectral characteristics of the KDE interval between 650-40 Ma of the ZHe record. Blue dashed line indicates the median smoothed spectrum (Meyers, 2014). Peaks are only identified if they satisfy both the ML96 robust red noise model (Mann and Lees, 1996) and MTM harmonic F-test at 85% and 90% confidence levels (e.g., Meyers, 2012).

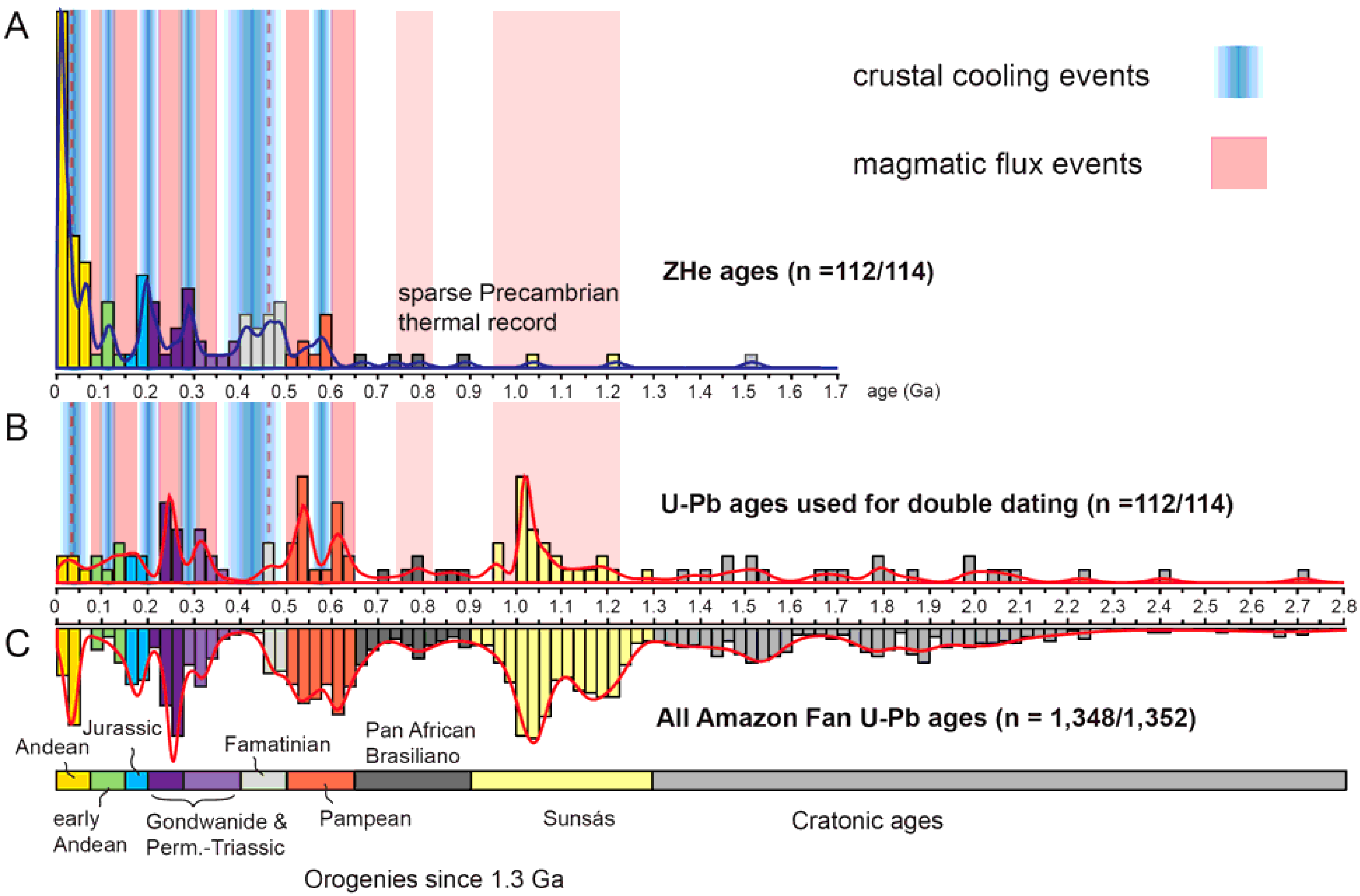

Figure 5

Kernel density estimates (KDEs) for detrital zircon U-Th/He age data and U-Pb age data from the Amazon fan. This figure highlights temporal relationships between periods of magmatic flux (colored red) and pulses of exhumation driven cooling (colored blue). A: KDE and histogram (25 Ma bins) for U-Th/He age data. B: KDE and histogram for U-Pb age data associated with cooling ages in part A. C: KDE and histogram for all published U-Pb DZ age data from the Amazon Fan (Mason et al., 2019).

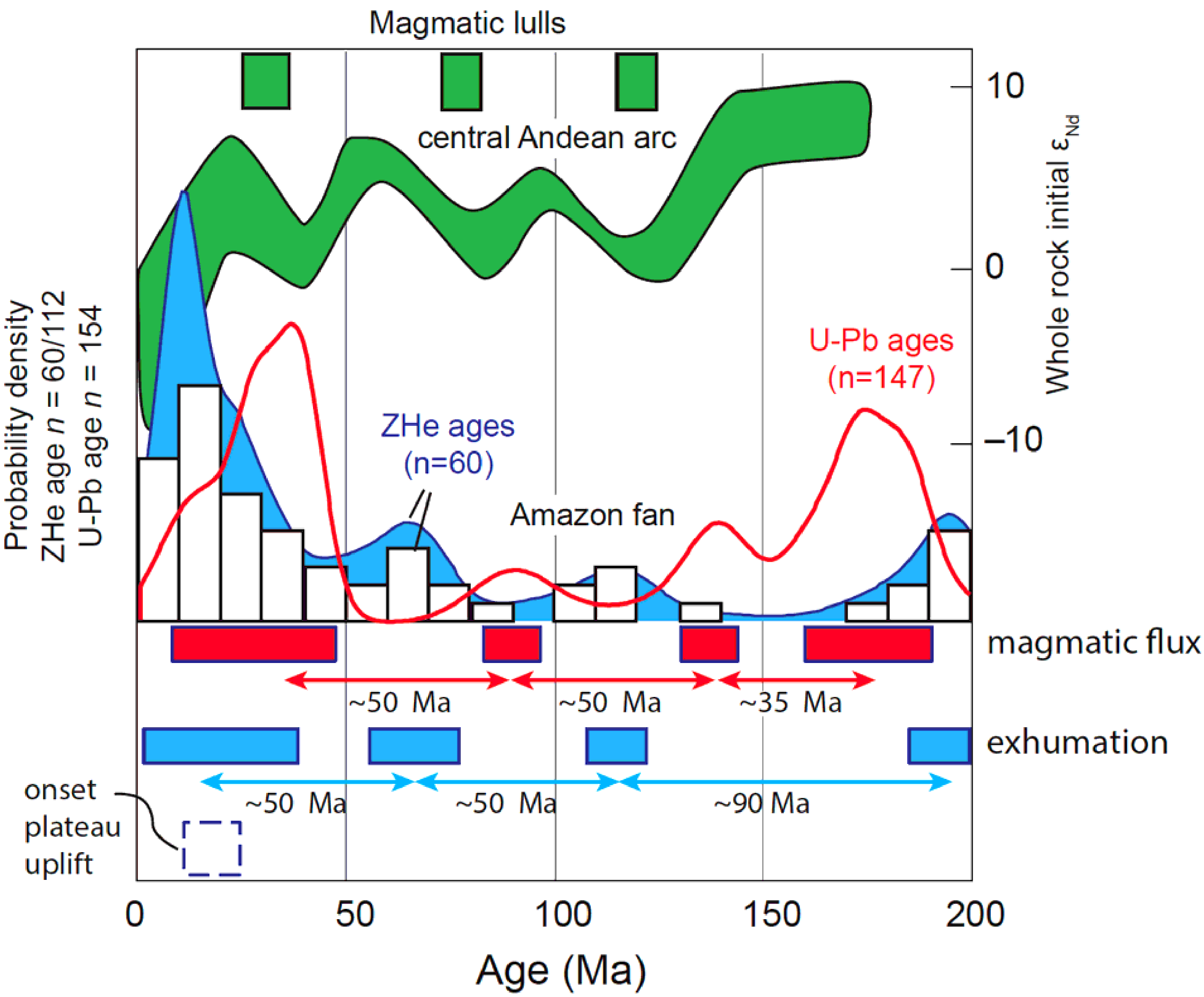

Figure 6

Summary of geochemical, geochronologic, and detrital thermochronologic data from the central Andes and Amazon Fan (modified from DeCelles et al., 2009). Top curve is whole rock neodymium values from the central Andean arc with interpreted magmatic lulls. Red unfilled KDE is U-Pb detrital zircon (DZ) ages from the Amazon Fan (Mason et al., 2019), blue filled KDE and histogram are DZ U-Th/He cooling ages from the Amazon Fan, with interpreted phases of high magmatic flux (red) and rapid exhumational cooling (blue) based on U-Pb and ZHe age data. Arrows with annotations delineate approximate periods of magmatic flux and exhumational cooling. Timing of Altiplano plateau uplift from Sundell et al., (2019).

Supplementary Files

This is a list of supplementary files associated with this preprint. Click to download.

- SupDataFileD1UThHeisotopicmeasurments.xlsx
- DescriptionofSupplementaryFilesforCyclesofAndeanMountainBuildingArchivedintheAmazonFan.docx